Role of Actuation in Combustion Control

J.P. Hathout, M. Fleifil, A. M. Annaswamy, and A.F. Ghoniem

Massachusetts Institute of Technology

Cambridge, MA 02139

March 13, 2001

Abstract

This paper presents analysis of the effect of actuation on combustion dynamics. Two different categories of actuators are examined: flow sources, e.g., acoustic speakers, and heat sources, e.g., fuel injectors. These sources are modeled in the conservation equations and a finite dimensional model is obtained. Two methods of analysis are used to gain insight into the physics of actuation, and its stabilizing/destabilizing effect on the combustor through feedback control. The first is the energy method which is used here in a novel way to explain work exchange between the different dynamic components of the system: the acoustics, the flame, and the actuator. Energy analysis is also used to quantify the "useful" and "wasted" work generated by actuators. The second method of analysis is the dynamic method in which the combustor is represented as an oscillator. This method is used as a basis of any optimal control design.

Nomenclature

A	combustor cross-sectional area	x_a	actuator location
c	speed of sound	x_f	flame location
D	combustor diameter	x_i	distance between injector and flame front
d_p	diameter of holes in a perforated disk	x_s	sensor location
E	acoustic energy flux	z_c	phase-lead controller zero
I	current input	α	decay rate
k	wave number	α_r	ratio of speaker membrane surface area to A
k_c	phase-lead controller gain	γ	specific heat ratio
k_d	stiffness of a diaphragm	Δh_r	enthalpy of reaction
k_l	speaker gain	Δ_L	difference over L
k_p	proportional controller gain	Δ_τ	difference over time, τ
L	combustor length	ζ	damping ratio
M	Mach number	$\eta(t)$	modal amplitude
m_d	diaphragm mass	θ	effect of velocity ahead and behind
$\hat{n}$	unit normal vector to the control volume		the flame on its dynamics
n_f	number of holes in a perforated disk	ρ	density
p	pressure	τ_i	convective time lag
p_c	phase-lead controller pole	Φ	rate of energy dissipation
S_u	burning velocity	ϕ	equivalence ratio
t	time	$\psi(x)$	modal amplitude
u	velocity	ω	mode frequency
v_c	flow source velocity	ω_l	speaker natural frequency
W	work	$(\cdot)'$	perturbed quantity
x	distance	$\overline{(\cdot)}$	mean quantity

1 Introduction

Combustion instability has been a major obstacle in designing and operating low-emission, lean premixed combustors, and high-powered, near stoichiometric combustors. Active control has shown promising results in abating the instability. Designing actuators depends on a clear in-

sight into the dynamics of the system, while optimizing its operation relies on the availability of accurate models of the dynamics as well as for how an actuator may impact it under a range of conditions.

The problem is critical in combustion instability since: (1) It is important to minimize the input energy through the actuator while recognizing certain practical limitations on its design such as its bandwidth and the power it delivers [1]; (2) while it is desirable to achieve the minimum possible settling time, this should be done without imposing unreasonable requirements on the actuator; (3) extra constraints on the design are usually encountered in practice, such as the allowable locations of the sensor and actuator, which may hinder achieving theoretically optimal conditions; and (4) since models are difficult to construct and validate, certain robustness is needed in the control design. Clearly, the role of an actuator and how it interacts with the system dynamics must be understood before these goals can be accomplished.

Models of combustion instability have been suggested [1]-[4]. However, effort to model the impact of the actuator on the system dynamics has been limited. In most cases, a simple relation is assumed to exist between the action of an actuator and the system response. For instance, when a speaker is employed, it is often assumed that its primary function is to introduce a pressure signal which counters the existing unstable pressure field (anti-sound). However, the subtle interactions between the actuator signal and the flame will be shown here to lead to different results depending on the structure of the control algorithm and its implementation into the system design, i.e. the locations of sensors and actuators, etc. We will also study the impact of an oscillating fuel stream.

In Section 2, thermoacoustic instability is reviewed using the traditional energy point of view, then alternatively, we show that adopting a system dynamics view can lead to significant insight into the features of an actuator. In Section 3, we present a finite dimensional instability model with different input actions from two different actuator categories, namely, (1) flow sources (e.g., speakers), and (2) heat sources (e.g., fuel injectors). The analysis of the impact of the former is performed in Section 4, while for the latter in Section 5 using a proportional and a phase-lead controller. In both sections, a dynamic analysis as well as an energy analysis are performed. We summarize in Section 6.

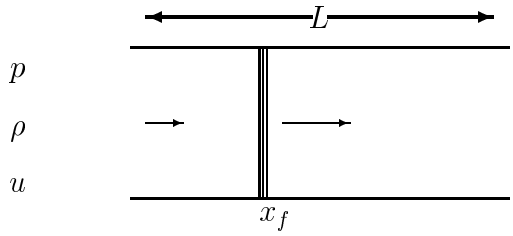

Figure 1: One dimensional reacting fluid flow with flame at $x = x_f$

2 Energy vs. Dynamics Analysis

In this section, we present two different but compatible approaches; namely the energy and dynamic analyses, for examining combustion instability in an organ-pipe combustor, which typically models situations of combustion in gas turbines and after-burners in applications. According to the first law of Thermodynamics, we start by carrying out an energy balance of the combustor. We note that the acoustic field (hosted by the combustor tube) is the primary energy storage mechanism in the combustor. Increasing or decreasing the stored (or internal) energy of this field can be achieved by transferring work or heat to the field. Since, in our case, the flame is considered a localized heat source, only a small control volume in the acoustic field is heated, the small volume expands and in turn exerts work on the field.

The acoustic energy density, e', in a one-dimensional acoustic field can be derived from the linearized conservation equations as (see [5], for more details)

$$e' = \frac{\overline{\rho} u'^2}{2} + \frac{p'^2}{2\overline{\rho c}^2}, \tag{1}$$

where ρ, u, and p are the density, velocity, and pressure in the field, respectively, $(.)'$ and $\overline{(.)}$ are the perturbed and mean values of the parameters, respectively, and $\overline{c}$ is the mean speed of sound. The first term in the RHS is the acoustic kinetic energy and the second is the potential or elastic acoustic energy. It is clear that any system that would sustain waves (also, as in many vibration processes) should have these two components of stored energy, and the periodic conversion from one form to the other sustains the oscillatory behavior.

The momentum and energy conservation equations for small perturbations in a combustor tube hosting a localized heat-release zone, as seen in Fig. 1, for zero mean velocity, $\overline{u}$, and for no spatial

gradients in the mean density, $\overline{\rho}$, pressure, $\overline{p}$, can be written as

$$\overline{\rho}\frac{\partial u'}{\partial t} + \frac{\partial p'}{\partial x} = 0, \tag{2}$$

$$\frac{\partial p'}{\partial t} + \gamma\overline{p}\frac{du'}{dx} = (\gamma - 1)q'. \tag{3}$$

By performing the operation $u'\times$(Eq. (2))+$\frac{p'}{\gamma\overline{p}}\times$(Eq. (3)), and using Eq. (1), we get

$$\frac{\partial e'}{\partial t} + u'\frac{\partial p'}{\partial x} + p'\frac{\partial u'}{\partial x} = \frac{\gamma - 1}{\overline{\rho c}^2}p'q'. \tag{4}$$

Integrating Eq. (4) spatially, over the length of the combustor, L, we get

$$\frac{\partial}{\partial t}\int_0^L e'Adx = \frac{\gamma - 1}{\overline{\rho c}^2}\int_0^L p'q'dx - \Delta_L(E'A) - \Phi, \tag{5}$$

where $E' = p'u'$, is the acoustic energy flux, Φ is the rate of energy dissipation. x, t are the distance and time, respectively, Δ_L signifies the difference over L, and A is cross-section area of the combustor. Equation (5) represents the Rayleigh criterion [6] which, for conditions satisfied by systems analyzed in this work, expresses the energy transfers in a continuous combustion system. The conclusion drawn from this condition is that a combustion system may become unstable when (1) $\angle(p' - q') \leq 90°$, i.e., when the magnitude of the first term in the RHS reaches high enough levels to overcome the dissipation and (2) when the energy flux terms (which are typically small in this class of combustors) add to the stored energy in the combustor at a rate faster than the dissipation.

In the case of a concentrated heat release zone, one may consider the boundaries between this zone and the acoustic field as virtual pistons which oscillate in phase with the oscillation of the heat deposition rate into the gas trapped between them. The work done by the oscillating pistons will add energy to the acoustic field. Viewed as such, the first term on the RHS of Eq. (5) can be written as a (pdV) work exchange between the small volume, V,within which heat is deposited and the acoustic field. The mass in this control volume undergoes a change in density which follows the heat release rate and leads to the expansion/contraction of the volume, against the fluctuating pressure at its boundaries. The effect of the flame on the acoustic field is therefore analogous to that of a flow source (e.g. speaker) which (as will be shown in Section 4.2) acting like a monopole [7], and the energy exchange between the flame and the acoustic field can be regarded as “work exchange”.

An equivalent, more revealing but less general statement can be obtained by expressing the pressure perturbation as a Galerkin expansion in time and space, $p'/\overline{p} = \Sigma\eta_i(t)\psi_i(x)$. Using the acoustic modes in the absence of heat addition, which satisfy the boundary conditions, to express the spatial dependence, one can develop equations governing $\eta_i(t)$. Assuming that one mode, whose amplitude is η, can be used to capture the dynamics adequately[1], and substituting in the equations governing the perturbation [3], the system response can be described by the following oscillator equation:

$$\ddot{\eta} + \omega^2\eta \;\; = \;\; \widetilde{b}\dot{q}', \tag{6}$$

where ω is the mode frequency, $\widetilde{b}$ is a constant which depends on the flame location. In Eq. (6), it is assumed that the heat release zone is compact, concentrated at a distance from the inlet of the combustor, and that dissipation is negligible. The oscillator equation is closed by expressing q' in terms of η and $\dot{\eta}$ (note that $\dot{\eta}$ is proportional to the velocity perturbation). We can assume, without loss of generality that $q' = q'(\dot{\eta})$ and for convenience write the above as

$$\ddot{\eta} + G(\dot{\eta})\,\dot{\eta} + \omega^2\eta \;\; = \;\; 0. \tag{7}$$

This equation shows that a combustion system becomes an unstable oscillator, i.e., possesses "negative damping", when $G(\dot{\eta}) < 0$. For small amplitudes, one can expand G and retain only the constant term to obtain the condition of the linear instability. One can show that this is equivalent to the Rayleigh criterion. As the perturbation grows, and making the reasonable assumption that combustion dynamics become nonlinear before acoustic dynamics, Eq. (7) can still be used to approximate the nonlinear behavior and the conditions and mechanisms responsible for establishing limit cycles. In this case, the dependence of G on $\dot{\eta}$, which is the only source of nonlinearity, must be retained.

3 Actuation in a Finite Dimensional Model

A finite dimensional model that includes both forms of actuation: speaker [8] and fuel injector [1] has been developed. Two mechanisms of combustion instabilities are reported in practical systems,

[1] Without external actuation, this assumption is valid. In case of external actuation, it may be necessary to use more than one mode [3].

the first is due to coupling of acoustics and heat release through flame-surface-area perturbations [2, 3] while the second is due to the coupling of acoustics and heat release oscillations through equivalence ratio perturbations [1, 4, 9, 10]. Experimental evidence of the former has been presented in [11, 12] while the latter has been observed in [13, 14, 15, 16]. We present the former form of instability in the analysis in this paper.[2] The final form of the finite-dimensional model is given by [3, 8]:

$$\ddot{\eta}_i + \omega_i^2 \eta_i = \widetilde{b}_i \, \dot{q}_f' + \widetilde{b}_{c_i} \, \dot{v}_c, \tag{8}$$

$$\dot{q}_f' + b_f q_f' = \omega_f \widetilde{g}_f \left(\frac{u_f'}{\overline{u}_f} + \frac{\phi_f'}{\overline{\phi}_f} + \frac{\dot{\phi}_f'}{\overline{\omega}_f \phi_f}\right), \tag{9}$$

$$u_f' = \Sigma_{i=1}^n \widetilde{c}_i \, \dot{\eta}_i + \alpha_r v_c, \tag{10}$$

$$p'(x,t) = \overline{p} \Sigma_{i=1}^n c_{c_i}(x) \eta_i(t), \tag{11}$$

where $\widetilde{b}_i = \gamma a_o \psi_i(x_f)/E$, $\widetilde{c}_i = \frac{1}{\gamma k_i^2} \frac{d\psi_i(x_f)}{dx}$, $\widetilde{b}_{c_i} = \gamma \alpha_r \psi_i(x_a)/E$, $c_{c_i} = \psi_i(x_s)$, $\omega_f = 4S_u/d_p$, $b_f = \omega_f(1 - \theta a_o \widetilde{g}_f)$, $a_o = (\gamma - 1)/\gamma\overline{p}$, $E = \int_0^L \psi_i \psi_i^T dx$, and $\widetilde{g}_f = n_f \rho \Delta h_r \overline{u}_f \overline{\phi}_f \, (d_p/D)^2$. Note that here we are modeling a premixed organ pipe type combustor of diameter D and length L with a perforated disk (with n_f holes of diameter d_p) acting as a flame holder [3]. γ, S_u and Δh_r are the specific ratio, the burning velocity and the enthalpy of reaction of the reactants, respectively. v_c and $\dot{v}_c$ are the velocity and acceleration of a typical flow source (e.g. a speaker), respectively, ϕ_f and u_f are the equivalence ratio and the velocity at the flame (out of a perforation), p is the pressure, $\overline{(.)}$ and $(.)'$ are the mean and perturbation of a variable. x_f, x_s, and x_a are the flame, the sensor (e.g., a microphone), and the flow source actuator (e.g., a speaker) locations measured from the upstream end, respectively. α_r is the ratio of the speaker membrane surface area to that of the duct cross section area. $\theta \in (0, 1)$ is a parameter expressing the effect of u_f' ahead and behind the flame on its dynamics [3]. k_i and E are the wave number and the energy in the mode, respectively.

[2] The instability triggered by equivalence-ratio fluctuations due to the convective time-delay is associated with a time-lag mechanism while that induced by flame surface area is due to a phase lag mechanism. In both cases, the phase relation between p' and q' is the same and hence the approach presented here is applicable to both cases.

4 The Role of a Speaker

4.1 Dynamic Analysis

Using a single mode to describe the acoustic dynamics, namely the unstable mode[3] we investigate how the loudspeaker impacts the combustor dynamics. For a single mode, Eqs.(8)-(10) are combined as follows:

$$\ddot{\eta}_1 - \widetilde{b}_1\omega_f\widetilde{g}_f\widetilde{c}_1\ \dot{\eta}_1 + \omega_1^2\eta_1 \quad = \quad \widetilde{b}_1\omega_f\widetilde{g}_{f_1}\alpha_r v_c + \widetilde{b}_{c_1}\ \dot{v}_c, \tag{12}$$

where $\widetilde{g}_{f_1} = \widetilde{g}_f/\overline{u}_f$. We neglect the second term on the LHS of Eq.(9), since the flame characteristic frequency is often an order of magnitude smaller than the acoustic frequency [2] (bulk modes may be exceptions to this rule, and are treated in [4]). Equations (8) and (12) show that the speaker affects the combustor dynamics through two parallel paths, a direct path through the pressure generated by its diaphragm acceleration, $\dot{v}_c$, and an indirect path through an additional component of unsteady heat release generated by its diaphragm velocity, v_c. If these two paths are managed, using an intelligent controller, so that they generate, collaboratively, "positive damping" that counters the "negative damping" induced by the unsteady heat release, the combustor can be stabilized. To achieve this "damping", both v_c and $\dot{v}_c$ must have components which are proportional to $\dot{\eta}_1$.

The dynamics of the diaphragm motion of a typical loudspeaker can be modeled as [7]:

$$\dot{v}_c + 2\zeta\omega_l v_c + \omega_l^2 \int v_c dt \quad = \quad k_l I, \tag{13}$$

where $\omega_l = \sqrt{k_d/m_d}$ is the natural frequency of the loudspeaker diaphragm, k_d and m_d are the equivalent stiffness and mass of the diaphragm, respectively, ζ is a damping ratio, k_l is a speaker gain, and I is the input current. We assume that $\omega_l < \omega_1$ which allows us to approximate the loudspeaker dynamics as

$$\dot{v}_c \quad \cong \quad k_l I. \tag{14}$$

The input current into the actuator is determined by a controller according to a measurement of

[3] Under certain conditions combustor control analysis may require more than one mode for accurate modeling [3]. For the sake of analytical tractability and to gain the requisite insight, we focus on cases where a single mode is sufficient.

p', u'_f or q'_f which is obtained via a sensor placed at a certain location in the combustor. In the following, we examine the impact of two different control algorithms.

4.1.1 A Proportional Controller:

The measured signal is chosen to be p' which is proportional to η_1, and we need either or both the source terms in the oscillator Eq. (12) to be proportional to $\dot{\eta}_1$. The simplest controller that can stabilize the system is a proportional controller for which the control input I is proportional to the sensor signal p', $I = k_p \overline{p} c_{c_1} \eta_1$. We compute $\dot{v}_c = k_l k_p \overline{p} c_{c_1} \eta_1$ and $v_c = k_l k_p \overline{p} c_{c_1} \dot{\eta}_1 / \omega_1^2$, where the approximate relation, $\eta_1 \cong -\ddot{\eta}_1 / \omega_1^2$ is used to get the later. The oscillator equation becomes

$$\ddot{\eta}_1 - \widetilde{b}_1 \omega_f \widetilde{g}_{f_1} \left(\widetilde{c}_1 - \alpha_r \frac{k_l k_p \overline{p} c_{c_1}}{\omega_1^2} \right) \dot{\eta}_1 + \left(\omega_1^2 - \widetilde{b}_{c_1} k_l k_p \overline{p} c_{c_1} \right) \eta_1 = 0. \tag{15}$$

Equation (15) shows that only the indirect path adds damping to the system. A stable oscillator must satisfy

$$\widetilde{b}_1 \omega_f \widetilde{g}_{f_1} \left(\widetilde{c}_1 - \alpha_r \frac{k_l k_p \overline{p} c_{c_1}}{\omega_1^2} \right) < 0. \tag{16}$$

The proportional controller has two free parameters: the sensor location which determines c_{c_1}, and the gain k_p, both of which have selectable signs. Thus, the controller has enough degrees of freedom to satisfy the inequality. Interestingly, the actuator location does not contribute to the damping, since it affects only the direct path. Although the proportional controller is able to add enough damping to achieve stability, it requires high gain since it takes advantage of a single channel only. Moreover, it changes the frequency of the oscillation substantially; part of the input energy is not utilized to suppress the instability. A large change in the frequency is expected, since $\widetilde{b}_{c_1} k_l k_p \overline{p} c_{c_1} > (\widetilde{b}_{c_1} \widetilde{c}_1 / \alpha_r) \omega_1^2$, and $(\widetilde{b}_{c_1} \widetilde{c}_1 / \alpha_r) \approx O(1)$. Thus, a fraction of the input energy, which will be quantified in Section 4.2, is ”wasted”.

The analysis shows some surprising results. While one traditionally considers the role of an acoustic actuator as a means of imposing a pressure signal which is out of phase with the existing signal, i.e., an anti-sound mechanism, our results here show that this is not always the case. In the case analyzed above, the only mechanism by which the actuator can impact the system is by affecting the heat source, through the extra velocity signal which is managed by the controller for stability.

4.1.2 A Phase-Lead Controller

To overcome the drawbacks in the proportional controller, one should design a controller such that both source terms in Eq.(8) contribute directly to $\dot{\eta}_1$. This can be achieved using a phase-lead compensator whose dynamics are governed by[4]:

$$\dot{I} + p_c I = k_c \overline{p} c_{c_1} \left(\dot{\eta}_1 + z_c \eta_1 \right), \tag{17}$$

where p_c, z_c, and k_c are the compensator parameters: pole, zero, and gain, respectively. In general, the quantity $p_c - z_c$ corresponds to the decay resulting from the damping effect that the phase lead controller provides, while k_c corresponds to the control effort needed to provide the damping. The phase-lead compensator adds a positive phase that can counter the "natural" negative phase, achieved via $p_c > z_c$ [17]. There are two choices for the compensator pole: $p_c > \omega_1$ and $p_c < \omega_1$. We discuss the first one only. In this case,

$$I \cong \frac{k_c \overline{p} c_{c_1}}{p_c} \left[\left(1 - \frac{z_c}{p_c} \right) \dot{\eta}_1 - \frac{\ddot{\eta}_1}{p_c} + z_c \eta_1 \right]. \tag{18}$$

Combining Eqs.(14) and (18), we write:

$$\dot{v}_c \cong \frac{k_o \overline{p} c_{c_1}}{p_c} \left[\omega_1 \left(\frac{z_c}{\omega_1} + \frac{\omega_1}{p_c} \right) \eta_1 + \left(1 - \frac{z_c}{p_c} \right) \dot{\eta}_1 \right], \tag{19}$$

which is integrated to

$$v_c \cong \frac{k_o \overline{p} c_{c_1}}{p_c} \left[\left(1 - \frac{z_c}{p_c} \right) \eta_1 - \frac{1}{\omega_1} \left(\frac{z_c}{\omega_1} + \frac{\omega_1}{p_c} \right) \dot{\eta}_1 \right], \tag{20}$$

where $k_o = k_l k_c$. Substituting in Eq. (12), we obtain:

$$\begin{aligned} \ddot{\eta}_1 &+ \left\{ -\widetilde{b}_1 \omega_f \widetilde{g}_{f_1} \widetilde{c}_1 + \frac{k_o \overline{p} c_{c_1}}{p_c} \left[\frac{\widetilde{b}_1 \omega_f \widetilde{g}_{f_1} \alpha_r}{\omega_1} \left(\frac{z_c}{\omega_1} + \frac{\omega_1}{p_c} \right) - \widetilde{b}_{c_1} \left(1 - \frac{z_c}{p_c} \right) \right] \right\} \dot{\eta}_1 \\ &+ \left\{ \omega_1^2 - \frac{k_o \overline{p} c_{c_1}}{p_c} \left[\widetilde{b}_{c_1} \omega_1 \left(\frac{z_c}{\omega_1} + \frac{\omega_1}{p_c} \right) - \widetilde{b}_1 \omega_f \widetilde{g}_{f_1} \alpha_r \left(1 - \frac{z_c}{p_c} \right) \right] \right\} \eta_1 = 0 \end{aligned} \tag{21}$$

The damping terms due to direct and indirect channels (the third and second term in the bracket multiplied by $\dot{\eta}_1$, respectively) show that the condition for the direct path to lead to positive damping is $\widetilde{b}_{c_1} k_o c_{c_1} < 0$, and that for the indirect path is $\widetilde{b}_1 k_o c_{c_1} > 0$. Recall that $\widetilde{b}_{c_1}$, $\widetilde{b}_1$, and c_{c_1} depend

[4] The phase-lead controller has enough dynamics to create terms in η_1 and its derivative $\dot{\eta}_1$. The latter is proportional to the velocity, u', and hence a similar control input can be obtained by sensing u' in addition to p', and modulating them through respective proportional controllers.

on the locations of the actuator, flame, and sensor, respectively, while k_o is the gain. The phase-lead controller has enough degrees of freedom to satisfy both inequalities at the same time, since we can choose $sign(k_o c_{c_1}) = sign(\widetilde{b}_1)$, and $sign(\widetilde{b}_{c_1}) = -sign(k_o c_{c_1})$.

To examine both effects in more detail, let k_o/p_c =const. In this case, the indirect damping decreases with p_c, while the direct damping increases. If the actuator is located close to a pressure node, where $\widetilde{b}_{c_1} = 0$, the indirect damping becomes dominant. The "optimization" of damping from both channels, i.e., achieving maximum total damping, is not well defined in the absence of actuator constraints, e.g., its location. For instance, when the actuator is close to a pressure node, then $z_c \approx \omega_1$ maximizes total damping. However, if we assume that k_o/p_c =const. and $z_c = 0$, maximum total damping is achieved when $p_c \approx \omega_1$. If the actuator is located at a pressure anti-node, maximum damping is achieved when the contribution from the direct and indirect paths are of the same order of magnitude. Similar results are obtained for $p_c < \omega_1$.

Thus, by properly selecting the controller parameters, one can impose damping through both channels and hence minimize the required input control energy for a given settling time.

4.1.3 Optimization

Here, we define optimization as minimizing "the maximum input power". Using $\mid \dot{\eta}_1 \mid \approx \omega_1 |\eta_1|$, we find, for $p_c > \omega_1$, that:

$$|I| \cong \frac{k_c \overline{p} c_{c_1} \omega_1}{p_c} \sqrt{\left(\frac{z_c}{\omega_1} + \frac{\omega_1}{p_c}\right)^2 + \left(1 - \frac{z_c}{p_c}\right)^2} |\eta_1| = P_d |\eta_1| \tag{22}$$

subject to the constraint that

$$\frac{k_o \overline{p} c_{c_1}}{p_c} \left[\frac{\widetilde{b}_1 \omega_f \widetilde{g}_{f_1} \alpha_r}{\omega_1} \left(\frac{z_c}{\omega_1} + \frac{\omega_1}{p_c}\right) - \widetilde{b}_{c_1} \left(1 - \frac{z_c}{p_c}\right) \right] = \text{const.} \tag{23}$$

The constraint comes from the fact that we need to minimize the input power for a certain settling time, and hence the damping coefficient must be held constant. Let $\frac{k_c}{p_c} = w_1$, $\frac{z_c}{\omega_1} + \frac{\omega_1}{p_c} = w_2$, $1 - \frac{z_c}{p_c} = w_3$, $\overline{p} c_{c_1} \omega_1 = g_1$, $k_l \overline{p} c_{c_1} \widetilde{b}_1 \omega_f \widetilde{g}_{f_1} \alpha_r / \omega_1 = g_2$ and $k_l \overline{p} c_{c_1} \widetilde{b}_{c_1} = -g_3$. The minimization problem is written as:

$$P_{d_{min}} \quad = \quad \min \left\{ w_1 g_1 \sqrt{w_2^2 + w_3^2} \right\}, \tag{24}$$

subject to

$$w_1(g_2 w_2 + g_3 w_3) \quad = \quad c_d, \tag{25}$$

leading to:

$$P_{d_{min}} \quad = \quad \frac{c_d g_1}{g_3} \min \left[\sqrt{\left(\frac{w_2}{w_3}\right)^2 + 1} \times \left(\frac{g_2 w_2}{g_3 w_3} + 1 \right)^{-1} \right]. \tag{26}$$

Equation (26) shows that the function to be minimized is reduced to a function in a single variable: (w_2/w_3). The minimum power is reached at

$$(w_2/w_3)_{min} \quad = \quad g_2/g_3, \tag{27}$$

and the minimum maximum amplitude of the input current is:

$$|I|_{min-max} \quad \cong \quad \frac{c_d g_1}{\sqrt{g_2^2 + g_3^2}} |\eta_1|_{max}. \tag{28}$$

It is worth noting that the optimal ratio in Eq. (27) leads to no change in the natural frequency of the oscillator in Eq.(21). Moreover, the problem of maximizing the damping while keeping the input power constant leads to the same result as in Eq. (27). Similar results are obtained for $p_c < \omega_1$.

To illustrate the optimization results, we test two controllers, an optimal and a non-optimal, with a combustor setup similar to Ref. [3]. The combustor is 4 cm in diameter and 50 cm long with closed upstream end and open downstream end. The flame is anchored on a perforated disc with 80 holes (each 1.5 mm in diameter), at x_f=32.5 cm. Assuming a perfect gas with $\gamma = 1.4$, $\overline{p}$ =1 atm, and Δh_r = 2.15$\times 10^6$J/kg, which corresponds to $\overline{\phi} = 0.7$, $S_u = 0.3$ m/s. Effects of the mean flow and mean heat addition are neglected. However, we include two acoustic modes (quarter and three quarter modes), the low frequency dynamics of the heat release, and the speaker dynamics (as in Eq. (13), with $k_l = 1404$, $\omega_l = 1822$, and $\zeta = 0.1$) in the combustor model. Since the analytical optimization result is based on one mode, we choose the sensor and actuator locations such that the coupling between modes is weak [3], namely we set x_s=1 cm and x_a=15 cm. Using the optimization analysis, we obtain $k_c = -0.1437,\ z_c = 2018.9$, and $p_c = 9173.2$. On the other hand, the second controller which is designed considering the phase needed for stability has $k_c = -0.1437,\ z_c = 100$, and $p_c = 15000$. We choose the gain of the latter to be equal to

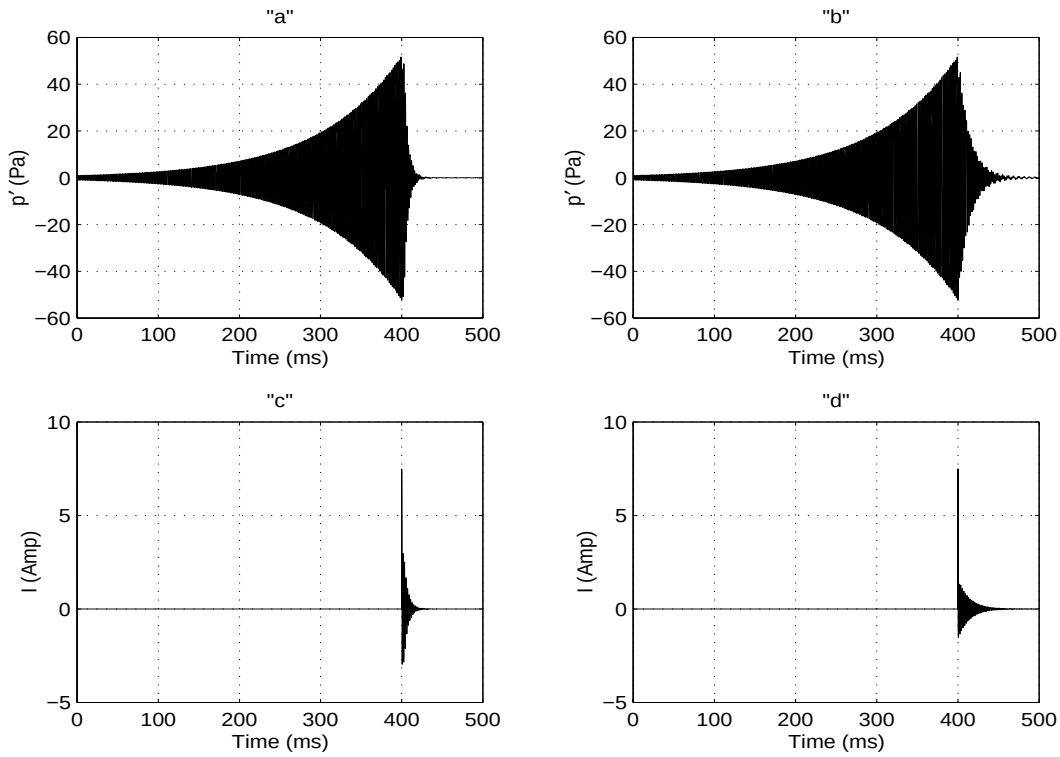

Figure 2: Controlled combustor responses. “a” and “c”: optimal, “b” and “d”: non-optimal

that of the optimal controller to ensure equal maximum input current. The pressure responses of the two controllers are shown in Figs. 2-a and 2-b (control is switched *on* at 400 ms). The control effort in terms of the speaker input current is given in Figs. 2-c and 2-d. One can see that for the same maximum input current, the optimal controller reduces the pressure to 5% of its initial value in 17 ms, while the non-optimal one needs 41.6 ms.

4.2 Energy Analysis

In Section 4.1, we based the stability analysis on the properties of the oscillator which models the combustor dynamics. Here, we pursue a different analysis for the purpose of explaining the origin of the “dissipation” in the oscillator equation. The primary energy storage mechanism in the combustor is the acoustic field. Increasing the stored (or internal) energy of this field can be achieved by doing positive work by “external” sources which include the flame and the actuator. Work done by the flame has been explained in Section 2 as work done on the field by expansion/contraction of a small volume surrounding the flame against negative/positive unsteady pressure. When actuation

using a speaker is incorporated and dissipation is neglected, the integral of Eq. (5) leads to

$$\begin{aligned}\Delta_\tau\left(\int_0^L e'dx\right) &= \frac{\gamma-1}{\overline{\rho}\overline{c}^2}\int_0^\tau\int_0^L p'q'dxdt \\ &\quad -\alpha_r\int_0^\tau\int_0^L p'\delta(x-x_a)\vec{v}_b.\hat{n}dxdt-\Delta_L\left(\int_0^\tau E'dt\right), \end{aligned} \tag{29}$$

where Δ_τ and Δ_L denote the change over time and over length, respectively, and we denote $\vec{v}_b = -v_c$, since the direction of the velocity from the speaker membrane is opposite to the unit normal to the control surface, $\hat{n}$, (note that the acoustic field is regarded here as the control volume). The RHS terms are the work per unit cross-section area of the combustor done by the heat source, in this case the flame, the speaker, and the net acoustic energy convected across the boundaries, respectively. The loudspeaker which is a flow source exerts work on the acoustic field similar to a monopole source [7].

Rewriting Eq. (29) as $\Delta_\tau\left(\int_0^L e'dx\right) = W_f + W_d$, substituting for the heat release dynamics using Eqs. (9) and (10), neglecting b_f with respect to the acoustics frequencies (as in Section 4.1), assuming the presence of one mode only, and carrying out the integration over L, we get

$$W_f = W_q + W_i, \tag{30}$$

$$W_q = \frac{\gamma-1}{\gamma}\omega_f\widetilde{g}_{f_1}c_{c_f}\widetilde{c}_1\int_0^\tau \eta_1^2 dt, \tag{31}$$

$$W_i = \frac{\gamma-1}{\gamma}\omega_f\widetilde{g}_{f_1}c_{c_f}\alpha_r\int_0^\tau \eta_1\left(\int_0^\tau v_b dT\right)dt, \tag{32}$$

$$\text{and } W_d = \alpha_r\overline{p}c_{c_a}\int_0^\tau \eta_1 v_b dt, \tag{33}$$

where Eqs. (31)-(33) denote the work exchange between the flame and the acoustic field; the actuator and the flame; and the actuator and the acoustic field directly, respectively. W_f is composed of the total work exchange with the flame. Without actuation, only W_q exists and work is done by the flame on the acoustic field. W_i arises because the speaker does work on the flame (through Eqs. (9) and (10)) and hence indirectly affects the acoustic field. This constitutes negative work on the field which counteracts W_q. W_d is work done by the field on the speaker.

Without active control,$W_d = W_i = 0$ and for an unstable combustor, $\Delta_\tau\left(\int_0^L e'dx\right) > 0$, and hence $W_f = W_q > 0$, while q'_f and p' are in phase. When active control is applied, the condition for stability, $\Delta_\tau\left(\int_0^L e'dx\right) < 0$, leads to $W_i + W_d < -W_q$.

For the proportional controller considered in Section 4.1.1, and for the conditions obtained by

the dynamic analysis (Eq. (16)), we find that

$$W_i = -\frac{\gamma-1}{\gamma}\omega_f \widetilde{g}_{f_1} \frac{\alpha_r k_l k_p \overline{p} c_{c_1} c_{c_f}}{\omega_1^2} \int_0^\tau \eta_1^2 dt < 0, \tag{34}$$

$$\text{and } W_d = \frac{\alpha_r k_l k_p \overline{p}^2 c_{c_1} c_{c_a}}{2\omega_1^2} \left[\eta_1^2(0) - \eta_1^2(\tau)\right] > 0. \tag{35}$$

Thus, as shown before, the impact of actuation which contributes to stabilization comes only from the indirect path while the direct path adds energy to the acoustic field. Moreover, since $W_i < -W_q$, $W_f < 0$, and q'_f and p' are out of phase. Actuation adds energy to the field from the direct channel, W_d, while it modifies the flame oscillations such that the work is done by the field on the flame ($W_f < 0$), and is so much larger than W_d that the overall effect is stabilizing.

The ratio of the "useful" work done by the loudspeaker, which stabilizes the combustor, and that wasted in the process, i.e., consumed in altering ω_1 as discussed in Section 4.1.1, is

$$\left|\frac{W_i}{W_d}\right| = 2\frac{\gamma-1}{\gamma}\frac{\omega_f \widetilde{g}_{f_1}}{\overline{p}} \left|\frac{c_{c_f}}{c_{c_a}}\right| \left|\frac{\int_0^\tau \eta_1^2 dt}{[\eta_1^2(0) - \eta_1^2(\tau)]}\right|, \tag{36}$$

$$\text{where } \left|\frac{\int_0^\tau \eta_1^2 dt}{[\eta_1^2(0) - \eta_1^2(\tau)]}\right| \cong \frac{1/\omega_1}{\alpha/\omega_1} = \frac{1}{\alpha}, \tag{37}$$

and α is the decay rate. This leads to $|W_i/W_d| \approx O(1)$. Thus, the useful work is of the same order as that wasted in changing the potential energy of the acoustic field. This ratio stays the same if q'_f is chosen as the feedback signal since $q'_f \propto \eta_1$. When $u'_f(\propto \dot{\eta}_1)$ is fed back, W_d becomes dominant.

When the phase-lead controller is used, for $p_c > \omega_1$ and maintaining the same stable conditions obtained from the dynamic analysis (Section 4.1.2), the work done per unit area is:

$$W_i \cong -\frac{\gamma-1}{\gamma}\omega_f \widetilde{g}_{f_1} \frac{\alpha_r k_o \overline{p} c_{c_1} c_{c_f}}{p_c \omega_1} \left(\frac{z_c}{\omega_1} + \frac{\omega_1}{p_c}\right) \int_0^\tau \eta_1^2 dt < 0, \tag{38}$$

$$\text{and } W_d \cong \frac{\alpha_r k_o \overline{p}^2 c_{c_1} c_{c_a}}{p_c} \left(1 - \frac{z_c}{p_c}\right) \int_0^\tau \eta_1^2 dt < 0. \tag{39}$$

Both forms of work exchange are done by the acoustic field on the actuator and the flame, i.e., actuation couples with the flame and the acoustic field to generate energy sinks for the acoustic field. Note that W_d in Eq. (39) is negative because of the choice of $sign(k_o c_{c_1}) = -sign(c_{c_a}) = sign(c_{c_f})$, in agreement with the stability conditions discussed in Section 4.1.2. Similar conclusions can be reached for the case with $p_c < \omega_1$. Thus, both the indirect and direct actuation paths

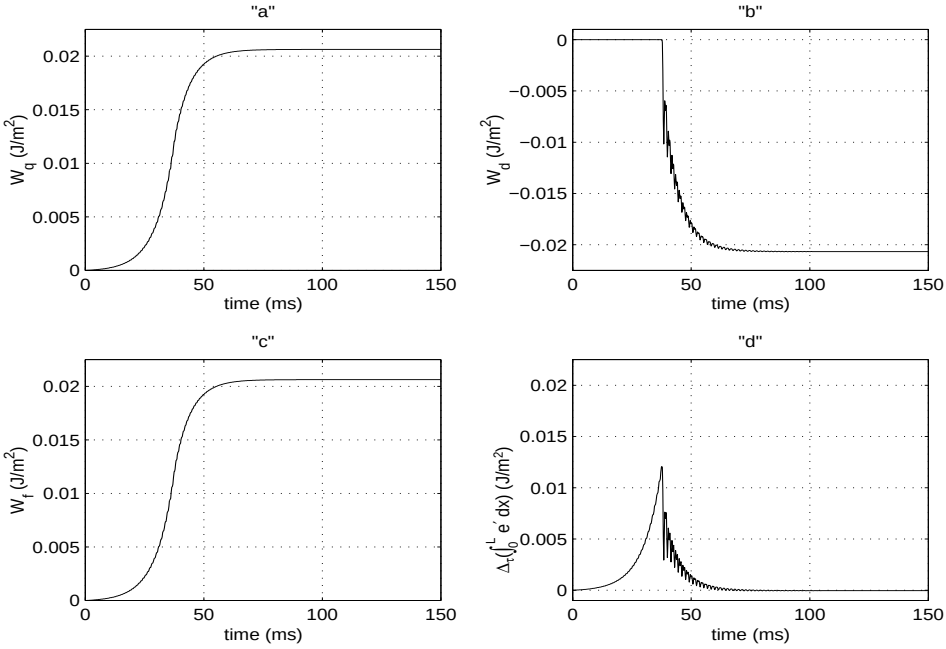

Figure 3: The different energy channels in the controlled combustor when only the direct effect is active, and the indirect effect is *forced* to zero

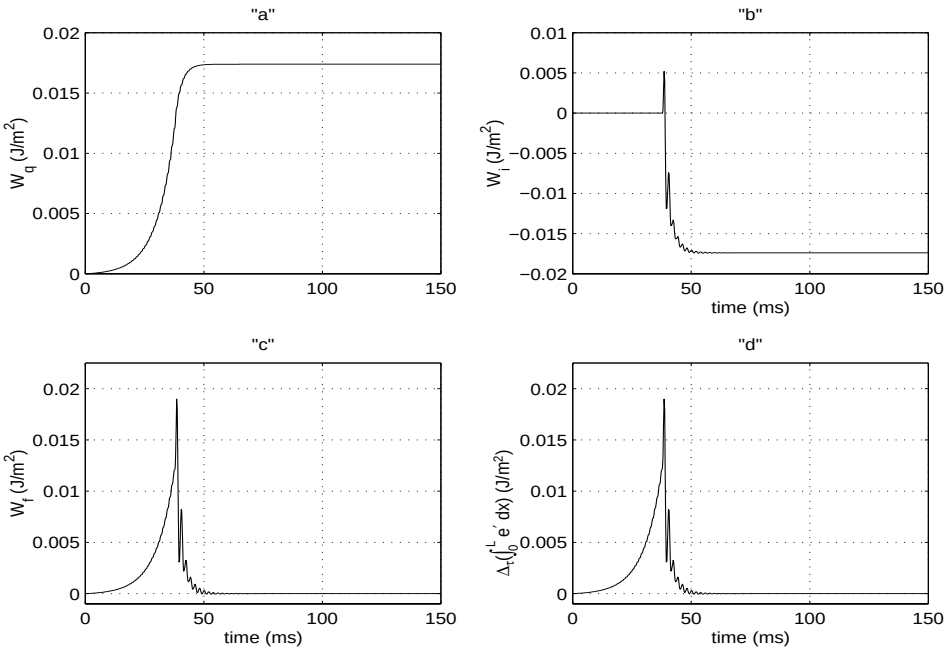

Figure 4: The different energy channels in the controlled combustor when only the indirect effect is active, and the direct effect is *forced* to zero

participate in decreasing the acoustic energy in the combustor. However, while the former mechanism changes the phase between q'_f and p' from $< 90°$ to $> 90°$, the latter appears as work done by the field on the actuator.

Figures 3 and 4 depict graphical representations of the results for a combustor similar to that described in Section 4.1.3 except for the values of x_f, x_a, and x_s, which are chosen as 24cm, 12.3cm, and 25cm, respectively. The controller parameters are $k_c = 250$, $z_c = 100$, and $p_c = 1000$ and make the direct and indirect work of the same order. Figure 3 shows the different energies for conditions when the indirect path is *forced* to zero. The latter can be weak if the flame is robust, i.e., is non responsive to fluctuations in the acoustic field. As shown in Fig. 3-d, the combustor is driven to stability when the control is turned *on* at 40ms, and the acoustic energy is reduced to zero. W_f (equivalent to the Rayleigh index) remains > 0 (Fig. 3-c), i.e., p' and q'_f remain in phase, whereas the energy sink stems completely from W_d (Fig. 3-b), i.e., the speaker extracts energy from the acoustic field. In Fig. 4, when the direct path is *forced* to zero, which can happen if the speaker is placed at a pressure node, $W_i < 0$ as shown in Fig. 4-b, i.e., p' and q'_f become out of phase, and W_f decreases as in Fig. 4-c. In this case also, the field does work on the speaker.

Using the optimal phase-lead controller designed in Section 4.1.3, we illustrate in Fig. 5 the different work exchanges. Note that W_d (Fig. 5-a) is dominant and contributes more to stabilization than W_i (Fig. 5-b). Thus, for this optimal controller, $W_f > 0$ (Fig. 5-c), i.e., p' and q'_f remain in phase. Figure 5-d shows that the combustor has been stabilized, and the acoustic energy is driven to zero.

The simulation illustrates that the different work exchanges affecting the acoustic energy maintain the same signs as predicted in the one-mode analysis, even in the presence of two modes and with no simplification in the heat release dynamics model (Eqs. (8)-(11)).

5 The Role of a Fuel Injector

In the case where an oscillating fuel stream (operated by a solenoid valve) is used for actuation, as in [18]-[21], we choose to inject the secondary fuel either at the burning zone, or upstream the flame where it mixes with the incoming mixture of reactants creating an unsteady equivalence ratio

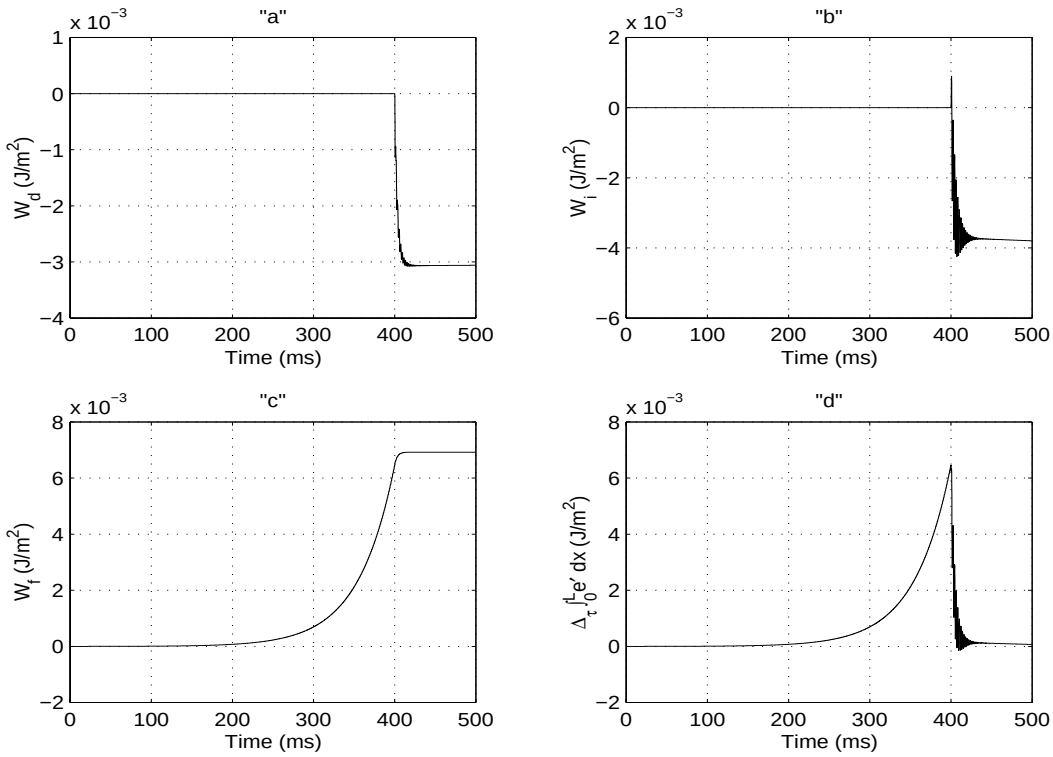

Figure 5: The different energy channels when the optimal phase-lead controller is used, as in Section 4.1.3

component, ϕ'. In the latter case, injection of a secondary fuel is done at a distance upstream the flame to guarantee good mixing. This introduces a convective time lag, τ_i, in ϕ' and the controlled equivalence ratio at the flame can be expressed as $\phi'_f(t) = \phi'(t - \tau_i)$, where $\tau_i = x_i/\overline{u}$; x_i is the distance between the injector and the flame front, and $\overline{u}$ is the mean velocity of the reactants. In most cases, τ_i is greater than the acoustic time constant of the system, $\tau = 2\pi/\omega$, ($\tau_i/\tau = kx_i/2\pi\overline{M}$, where k is the wave number and $\overline{M}$ is the Mach number), and conventional control techniques will fail to stabilize the system [17]. Several studies have proposed control solutions for systems with large delays [22, 23] and the implementation of these schemes is described in other articles [1, 4, 9]. In this paper, we will analyze the case when injection is done at the flame zone [18]-[20], thus minimizing transport lag.

5.1 Dynamic Analysis

Equations (8)-(10) are combined to derive the oscillator equation:

$$\ddot{\eta}_1 - \tilde{b}_1\omega_f\tilde{g}_{f_2}\tilde{c}_1\ \dot{\eta}_1 + \omega_1^2\eta_1 \quad = \quad \tilde{b}_1\omega_f\tilde{g}_{f_2}(\phi'_f + \dot{\phi}'_f\ /\omega_f), \tag{40}$$

where $\tilde{g}_{f_2} = \tilde{g}_f/\overline{\phi}_f$. The combustion system, through the heat release dynamics, Eq. (9), reacts to equivalence ratio perturbations, and its rate of change [1, 4, 9]. It is clear that if ϕ'_f is modulated in such a way to create positive damping that would counteract the destabilizing damping caused by heat release, stability can be reached. For the purpose of this paper, the dynamics of the injector will be disregarded for simplicity (see [1] for analysis of injector dynamics) assuming that the bandwidth of the injector is much higher than the acoustic frequencies. Therefore, we assume $\phi'_f \cong k_i I$. Using a pressure transducer as sensor, consistent with the analysis done with the speaker in Section 4, the signal fed to the controller is proportional to η_1.

5.1.1 A Proportional Controller:

A proportional control is the simplest structure that can be used to stabilize the combustor. Similar to Section 4.1.1, the equivalence ratio at the burning zone is written as $\phi'_f = k_i k_p \overline{p} c_{c_1}\eta_1$, with its rate of change $\dot{\phi}'_f = k_i k_p \overline{p} c_{c_1}\ \dot{\eta}_1$, and hence the oscillator becomes

$$\ddot{\eta}_1 - \tilde{b}_1\omega_f\tilde{g}_{f_2}\left(\tilde{c}_1 - \frac{k_i k_p \overline{p} c_{c_1}}{\omega_f}\right)\dot{\eta}_1 + \left(\omega_1^2 - \tilde{b}_1\omega_f\tilde{g}_{f_2}k_i k_p \overline{p} c_{c_1}\right)\eta_1 = 0. \tag{41}$$

Eq. (41) shows that there are two channels through which the actuation input due to fuel injection affects the dynamics, where the first is due to the effect of ϕ'_f, and the other is due to $\dot{\phi}'$. Both inputs are affected by the dynamics of the controller used. Hence, both could be sources of positive damping similar to the direct and indirect effects in the speaker case. The equivalence ratio (at the heat release zone) has a dynamic effect because the input from the injector is ”filtered” through the flame area dynamics, heat release dynamics, and acoustics dynamics. It should be noted that the rate of heat release is the primary effect on the acoustics dynamics which in turn is strongly affected by the rate of change of the equivalence ratio. The reader is referred to [9, 1, 4] for further details regarding fuel-injection dynamics.

Thus only $\dot{\phi'}_f$ adds damping to the system, whereas the ϕ'_f channel contributes only in changing the frequency at which the system oscillates. The condition for stability is

$$\widetilde{b}_1 \omega_f \widetilde{g}_{f_2} \left(\widetilde{c}_1 - \frac{k_i k_p \overline{p} c_{c_1}}{\omega_f} \right) < 0. \tag{42}$$

The proportional controller has enough degrees of freedom to stabilize the system. These are the sensor's location, c_{c_1}, and the gain, k_p, both of which have selectable signs. We note that unlike the speaker in Section 4.1.1, the "wasted" effort is much smaller, and can be estimated using Eqs. (41) and (42) as $\widetilde{b}_1 \omega_f \widetilde{g}_{f_2} k_i k_p \overline{p} c_{c_1} > \omega_1$ which is less than ω_1^2 by $O(\omega_1)$. In section 5.2, this "wasted" energy will be estimated as a fraction of the "useful" energy.

5.1.2 A Phase-Lead Controller:

For the case when $p_c > \omega_1$, a phase-lead controller can be approximated as described in Eq. (18), with ϕ'_f replacing $\dot{v}_c$ in Eq. (19), and $k_o = k_i k_c$. The rate of equivalence ratio variation becomes:

$$\dot{\phi'}_f \cong \frac{k_o \overline{p} c_{c_1}}{p_c} \left[\omega_1^2 \left(1 - \frac{z_c}{p_c} \right) \eta_1 + \omega_1 \left(\frac{z_c}{\omega_1} + \frac{\omega_1}{p_c} \right) \dot{\eta}_1 \right]. \tag{43}$$

Substituting in Eq. (40) leads to:

$$\begin{aligned} \ddot{\eta}_1 \quad &+ \quad \left\{ -\widetilde{b}_1 \omega_f \widetilde{g}_{f_2} \widetilde{c}_1 - \widetilde{b}_1 \omega_f \widetilde{g}_{f_2} \frac{k_o \overline{p} c_{c_1}}{p_c} \left[\omega_1 \left(\frac{z_c}{\omega_1} + \frac{\omega_1}{p_c} \right) + \left(1 - \frac{z_c}{p_c} \right) \right] \right\} \dot{\eta}_1 \\ &+ \quad \left\{ \omega_1^2 - \widetilde{b}_1 \omega_f \widetilde{g}_{f_2} \frac{k_o \overline{p} c_{c_1}}{p_c} \left[\omega_1 \left(\frac{z_c}{\omega_1} + \frac{\omega_1}{p_c} \right) - \omega_1^2 \left(1 - \frac{z_c}{p_c} \right) \right] \right\} \eta_1 = 0. \end{aligned} \tag{44}$$

We note that both channels contribute to "positive" damping when the condition for stability $\widetilde{b}_1 k_o c_{c_1} < 0$, and hence $sign(k_o c_{c_1}) = -sign(\widetilde{b}_1)$, is satisfied.

As in the case of a proportional controller, some energy is wasted in changing the frequency of the oscillator, and this can be estimated following arguments similar to 4.1.2 for the speaker. In order to force the injector to target all the effort towards adding damping without waste in changing the potential energy of the system, i.e., ω_1, an optimal approach similar to Section 4.1.3 can be utilized. As discussed before, the optimization will lead to zero change in the natural frequency. In the following, we quantify both analytically and graphically the energy exchanges between the injector's inputs, $\dot{\phi'}_f$ and ϕ'_f, and the combustor which cause positive damping.

5.2 Energy Analysis

The energy balance equation for a combustor with an unsteady fuel injector, assuming no external dissipation is identical to Eq.(29) without the second term in the RHS (which is due to the speaker). The only means for stabilizing a combustor using a secondary fuel injector is to affect the phase between q'_f and p', similar to the indirect actuation in the speaker (Section 4.2). Because of the linearity of the problem, one can identify easily the work contributed by actuation, W_{inj}, and by the acoustic field, W_q, to the total work, W_f, as follows:

$$W_f = W_q + W_{inj}, \tag{45}$$

$$W_{inj} = W_\phi + W_{\dot{\phi}}, \tag{46}$$

$$W_\phi = \frac{\gamma-1}{\gamma}\omega_f \widetilde{g}_{f_2} c_{c_f} \int_0^\tau \eta_1 \left(\int_0^\tau \phi'_f dT\right) dt, \tag{47}$$

$$\text{and } W_{\dot{\phi}} = \frac{\gamma-1}{\gamma}\omega_f \widetilde{g}_{f_2} c_{c_f} \int_0^\tau \frac{\phi'_f}{\omega_f}\eta_1 dt, \tag{48}$$

As discussed in Section 5.1, the injector has two contributions: one from the equivalence ratio and the other from its rate of change; they are denoted here as W_ϕ, and $W_{\dot{\phi}}$, respectively. When no active control is implemented, $W_q > 0$ (and is defined in Eq. (31)), the energy in the combustor grows according to Eq. (29). Thus, the for stability, negative work must be introduced using ϕ'_f in order to satisfy $W_{inj} < -W_q$.

As discussed in Section 5.1, using a proportional controller, only $\dot{\phi}_f$ can be made to contribute to stability. This can be illustrated also in terms of the work done per unit area where:

$$W_{\dot{\phi}} \cong \frac{\gamma-1}{\gamma}\omega_f \widetilde{g}_{f_2} k_i k_p \overline{p} c_{c_1} \int_0^\tau \eta_1^2 dt < 0, \tag{49}$$

$$\text{and } W_\phi \cong \frac{\gamma-1}{\gamma}\frac{\omega_f \widetilde{g}_{f_2} k_i k_p \overline{p} c_{c_1}}{2\omega_1^2}[\eta_1^2(0) - \eta_1^2(\tau)] > 0. \tag{50}$$

The ratio of the useful work, targeted towards dissipative energy, to the work wasted in changing the potential energy of the system can be estimated by considering Eqs. (49) and (50), with (37), as

$$\left|\frac{W_{\dot{\phi}}}{W_\phi}\right| \cong \frac{2\omega_1^2}{\omega_f}\frac{1}{\alpha} \cong O\left(\frac{\omega_1}{\omega_f}\right) > 1. \tag{51}$$

In this case, unlike the case of the speaker (Section 4.2), the useful work of the injector is larger than the wasted one, supporting the results in the dynamic analysis in Section 5.1.1.

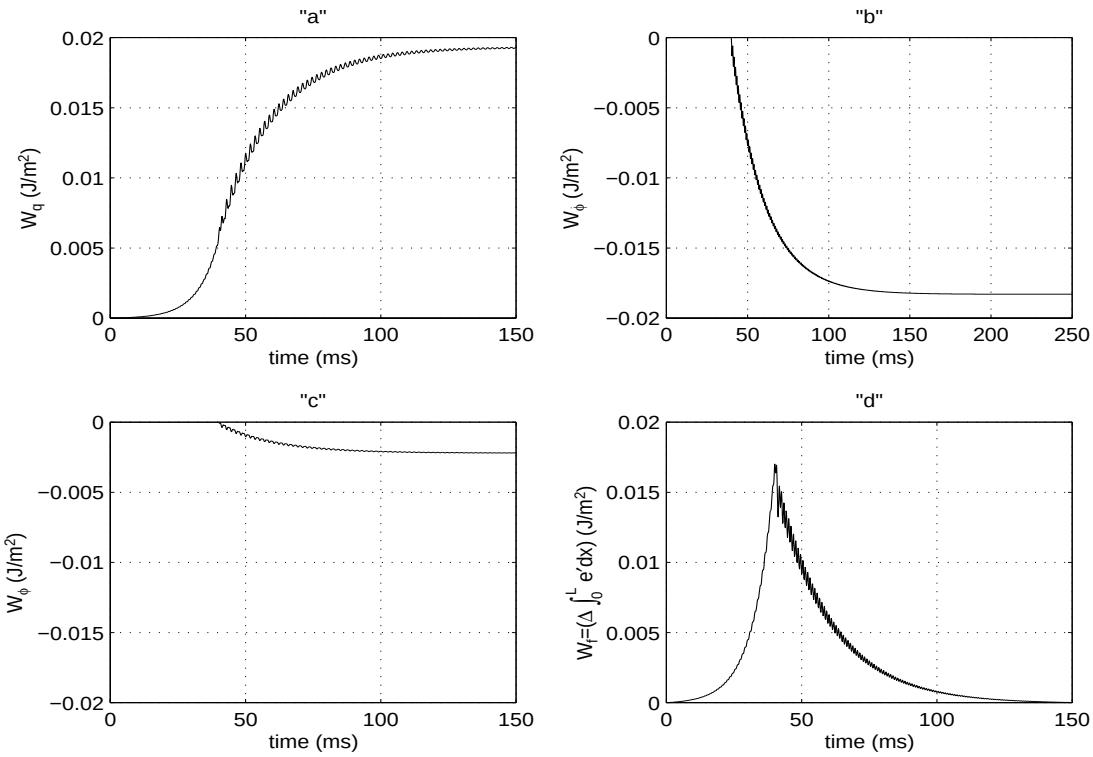

Figure 6: The different energy channels in the controlled combustor when using a fuel injector.

The phase-lead controller, discussed in Section 5.1.2, has sufficient degrees of freedom to accomplish stability, and one can show that

$$W_{\dot{\phi}} \cong \frac{\gamma-1}{\gamma}\omega_f \tilde{g}_{f_2} \frac{k_o \overline{p} c_{c_1} c_{c_f}}{p_c \omega_f}\left(\frac{z_c}{\omega_1}+\frac{\omega_1}{p_c}\right)\int_0^\tau \eta_1^2 dt < 0, \tag{52}$$

$$\text{and } W_\phi \cong \frac{\gamma-1}{\gamma}\omega_f \tilde{g}_{f_2} \frac{k_o \overline{p}^2 c_{c_1}}{p_c}\left(1-\frac{z_c}{p_c}\right)\int_0^\tau \eta_1^2 dt < 0. \tag{53}$$

Although both $W_{\dot{\phi}}$ and W_ϕ contribute in stabilizing the combustor, the former effect is larger than the latter, and this can be quantified as

$$\left|\frac{W_{\dot{\phi}}}{W_\phi}\right| = \frac{\left(\frac{z_c}{\omega_1}+\frac{\omega_1}{p_c}\right)}{\left(1-\frac{z_c}{p_c}\right)}\frac{\omega_1}{\omega_f} \sim O(10). \tag{54}$$

Figure 6 is a graphical representation of the analytical results. The phase-lead parameters are $k_c = 2000$, $z_c = 100$ and $p_c = 1000$. Both channels, $W_{\dot{\phi}}$ (in Fig. 6-b) and W_ϕ (in Fig. 6-c), suppress the instability by doing work on the heat release such that the phase between q'_f and p' is modified to ¡$90°$, similar to the indirect effect in a speaker. It is worth noting, from Fig. 6 b and c, that $W_{\dot{\phi}}/W_\phi \sim O(10)$ as estimated by Eq. (54).

6 Summary

The impact of two different types of actuators; flow and heat source actuators, which are most commonly used for abating combustion instability, are analyzed using two different approaches. First, a typical flow source actuator; an acoustic speaker, is studied. The dynamic analysis reveals how controlled actuation introduces dissipation, and is used to obtain the criteria for stability in terms of the controller parameters, the sensor/actuator locations, and the combustor parameters. The energy analysis is then carried out to relate the dissipative terms to the work done by/on the speaker. The speaker is found to exchange work with the acoustic field directly, and indirectly through the flame. One can quantify these energy transfers, define their physical origins, and determine the necessary control signals to the actuators for minimizing the acoustic energy in the combustor. Controller optimization analysis is performed based on the physical insight gained from the dynamic analysis of the combustor.

A heat source actuator in the form of a fuel injector is then analyzed dynamically as well as energetically. The work exchange between the injector and the acoustic field is shown to resemble the indirect work exchange between the speaker and the acoustic field, since both actions affect the acoustics through modulating the flame. The results presented herein shed more light on the physics behind the different actuation effects, and emphasize the importance of using this understanding in designing effective actuators and stabilizing optimal controllers.

7 Acknowledgements

This work is sponsored in part by the National Science Foundation, contract no. ECS 9713415, and in part by the Office of Naval Research, contract no. N00014-99-1-0448.

References

[1] J. P. Hathout, A. M. Annaswamy, and A. F. Ghoniem. Modeling and control of combustion instability using fuel injection. In *AVT Nato Conference*, Braunschweig, Germany, May 8-12 2000.

[2] M. Fleifil, A. M. Annaswamy, Z. Ghoniem, and A. F. Ghoniem. Response of a laminar premixed flame to flow oscillations: A kinematic model and thermoacoustic instability result. *Combust. Flame*, 106:487–510, 1996.

[3] A. M. Annaswamy, M. Fleifil, J. P. Hathout, and A. F. Ghoniem. Impact of linear coupling on the design of active controllers for thermoacoustic instability. *Combust. Sci. Tech.*, 128:131–180, 1997.

[4] M. Fleifil, J.P. Hathout, A.M. Annaswamy, and A.F. Ghoniem. "Reduced order modeling of heat release dynamics and active control of time-delay instability". *AIAA 2000-0708, 38th AIAA Aerospace Sciences Meeting, Reno, NV, 10-13 January*, 2000.

[5] A.P. Dowling and J.E. Ffowcs-Williams. *Sound and Sources of Sound*. Ellis Horwood Limited, West Sussex, PO191EB, England, 1983.

[6] J.W.S. Rayleigh. *The Theory of Sound*, volume 2. Dover, New York, 1945.

[7] P.A. Nelson and S.J. Elliott. *Active Control of Sound*. Academic Press, London, England, 1994.

[8] M. Fleifil, J. P. Hathout, A. M. Annaswamy, and A. F. Ghoniem. The origin of secondary peaks with active control of thermoacoustic instability. *Combustion, Science, and Technology*, 133:227–265, 1998.

[9] J. P. Hathout, M. Fleifil, A. M. Annaswamy, and A. F. Ghoniem. Heat-release actuation for control of mixture-inhomogeneity-driven combustion instability. In *28th International Symposium on Combustion*, University of Edinburgh, Scotland, July 30-August 4, 2000.

[10] T. Lieuwen, Y. Neumeier and B.T. Zinn. The role of unmixedness and chemical kinetics in driving combustion instabilities inlean premixed combustors. *Combust. Sci. Tech.*, vol. 135, pp.193-211, 1998.

[11] K. K. Venkataraman, L. H. Preston, D. W. Simons,B. J. Lee, J. G. Lee,and D. A. Santavicca. Mechanism of combustion instability in a lean premixed dumb combustor. *Journal of Propulsion and Power*, vol. 15, no.6, pp.909-918, December, 1999.

[12] S. Ducruix, D. Durox and S. Candel. Theoretical and experimental determinations of the transfer function of a laminar premixed flame. In *28th International Symposium on Combustion*, University of Edinburgh, Scotland, July 30-August 4, 2000.

[13] T. Lieuwen and B.T. Zinn. The Role of Equivalence Ratio Oscillations in Driving Combustion Instabilities in Low $N0_X$ Gas Turbines. In *27th International Symposium on Combustion*, pp. 1809-1816, 1998.

[14] T. Lieuwen and B.T. Zinn. Theoretical investigation of combustion instability mechanisms in lean premixed gas turbines. In *36th AIAA Aerospace Sciences Meeting, Reno, NV*, 1998.

[15] G.A. Richards and M.C. Janus. Characterization of oscillations during premixed gas turbine combustion. *Transactions of the ASME*, vol. 120, pp. 294-302, 1998.

[16] T. Lieuwen, H. Torres, C. Johnson and B.T. Zinn. A mechanism of combustion instability in lean premixed gas turbine conbustors. In *International Gas Turbine and Aeroengine Congress and Exhibit, Indianapolis, IN*, 1999.

[17] K. Ogata. *Modern Control Engineering*. Third Edition, Prentice Hall, Inc., NJ, 1997.

[18] K. R. McManus and J. C. Magill. Control of thermo-acoustic instabilities using pulse width modulation. *Proceedings of the 1997 IEEE Int'l Conf. on Control Applications*, pages 824–829, 1997.

[19] K. Yu, K.J. Wilson, and K.C. Schadow. Active combustion control in a liquid-fueled dump combustor. In *35th Aerospace Sciences Meeting and Exhibit*, pages AIAA 97–0462, Reno, NV, 1997.

[20] J.R. Seume, N. Vortmeyer, W. Krause, J. Hermann, C.-C Hantschk, P. Zangl, S. Gleis, and D. Vortmeyer. "Application od active combustion instability control to a heavy-duty gas turbine". In *Proceedings of the ASME-ASIA*, Singapore, 1997.

[21] J. M. Cohen, N. M. Rey, C. A. Jacobson, and T. J. Anderson. "Active control of combustion instability in a liquid-fueled low-NO_x combustor". *ASME 98-GT-267, ASME/IGTI, Sweden*, 1998.

[22] K. Ichikawa. Frequency-domain pole assignement and exact model-matching for delay systems. *Int. J. Control*, 41:1015–1024, 1985.

[23] S. I. Niculescu and A. M. Annaswamy. A simple adaptive controller for positive-real systems with time-delay. In *The American Control Conference in Chicago, IL.*, February 2000.